

05.1

Temporal pattern of microcracking in impact–damaged porous SiC ceramics

© I.P. Shcherbakov, A.G. Kadomtsev, A.E. Chmel

Ioffe Institute, St. Petersburg, Russia
E-mail: chmel@mail.ioffe.ru

Received January 18, 2022

Revised March 21, 2022

Accepted April 20, 2022

Temporal characteristics of the localized damage development initiated by a short–time impact pointed loading of SiC ceramics which is widely applied as a protective material against the shock action upon engineering constructions and people were investigated. The statistics of crack nucleation and relaxation was studied with the methods of acoustic emission and electromagnetic emission, correspondingly. It was shown that the length of intervals between microcrack nucleations follows a power law specific to cooperative phenomena. The time distribution of decaying electric charges which appear on impact–induced crack edges and annihilate after the passage of impact wave was, in contrast, linear. The temporal pattern of the crack relaxation permitted identifying two sets of newly formed damages that are the tiny cracks localized in the grain bulk and those that interconnect grains.

Keywords: SiC, porous ceramics, impact damage, acoustic emission, electromagnetic emission.

DOI: 10.21883/TPL.2022.06.53463.19140

Mechanical behavior of porous ceramics significantly depends on two microstructure factors, namely, the size of sintered grains and pore volume [1–3]. The ratio of these parameters defines the ceramics heterogeneity that governs the material deformation and damage (beginning from nucleation and development of primary defects under an external force impact). In loaded heterogeneous materials characterized by a great number of conditionally „weak“ points, catastrophic damage is preceded by accumulation of multiple microcracks, which passes to the stage of clustering and, then, to the loss of mechanical stability. The stage of local defects accumulation may be statistically characterized by energy releases during the acts of crack nucleation and also by time intervals between them. The temporal aspect of the damage evolution is especially interesting in the case of impact loading of the SiC ceramics, since its application area [4] embraces protections against shock impacts on humans and engineering structures [5], as well as on composite armors [6].

This paper presents temporal characteristics of the destruction evolution in the porous SiC ceramics damaged by a shock impact. The characteristics were obtained by the methods of acoustic emission (AE) and electromagnetic emission (EME), which enable estimating the statistics of the defect formation and relaxation at the microstructure level. In the process of formation of microcracks whose nucleation and development manifest themselves in AE pulse generation, layers of opposite electrical charges arise at the opposite crack edges due to wall chipping, friction and sliding [7].

Cracks relaxation after the shock wave passage causes annihilation of the formed charges with emission of electromagnetic signals [8]. In this study we have analyzed

distributions of time intervals between pulses in the AE and AME pulse series (i. e. „waiting times“ for the next pulse) and revealed the structure of microcrack „life cycles“ from nucleation to collapsing.

The samples were fabricated by sintering ultradispersed SiC powder with the particle size of $\sim 0.2\ \mu\text{m}$. Porosity of the silicon carbide ceramics may be varied by adding certain sintering additives [9,10]. In our case, those additives were Al_2O_3 (6.5 and 10.8 wt.%), B and C (2.5 and 6.8 wt.%); the sintering temperature ranged from 1920 to 2250°C. As a result, ceramics with porosity (P) of 1% (sample SiC1) and 9% (SiC9) were prepared.

In the experiments, samples in the form of plates 1 mm thick were placed on a heavy solid support coated with a layer of consistent lubricant. The impacts were performed with a hardened–steel tapered peen on which a 100 g weight was fallen from the height of 70 cm. The damages had the shape of small craters up to ~ 0.2 mm in diameter.

Temporal series of AE damages were detected by using a wide–band detector made from high–sensitive ceramics $\text{Pb}(\text{Zr}_x\text{Ti}_{1-x})\text{O}_3$, which was fixed on the sample with viscous glue. The EME signal was received by a Hertzian dipole. Emission signals of both types were transmitted to the analog–to–digital converter and saved in a computer. The emission detection was started at the moment when the peen got in contact with the sample surface; the time series durations were 1 ms. The limiting frequency of the detected signals was 1 MHz. To cut off the foreign noise contribution of the experimental setup vibrations, AE signals were subjected to low–frequency digital discrimination at the level of 80 kHz.

Time sweeps of amplitudes of AE pulses generated by the impact are presented in Fig. 1. The interpulse

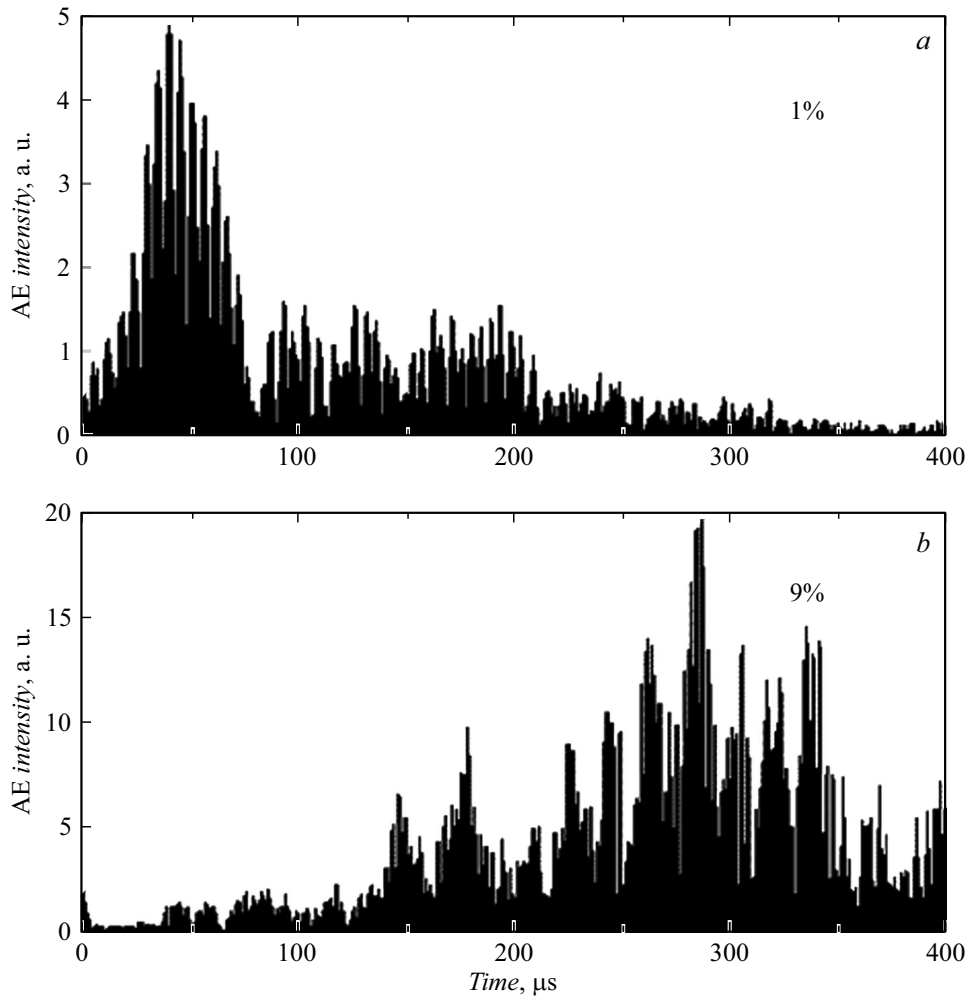


Figure 1. Time time sweeps of AE pulses initiated by impact loading of SiC ceramics with the porosity of 1 (a) and 9% (b).

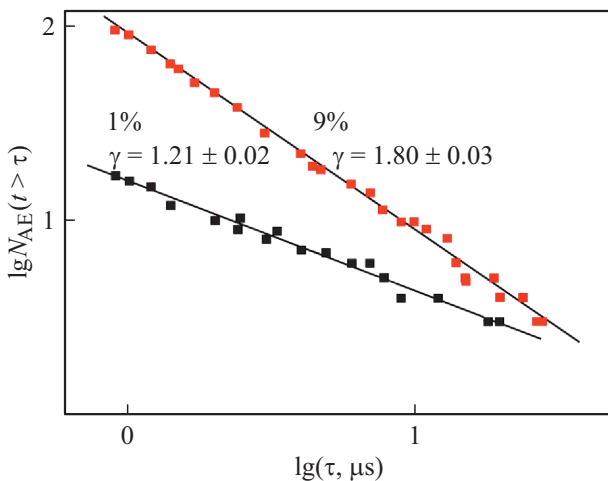


Figure 2. Distributions of time intervals between AE pulses induced by an impact load in SiC ceramics with porosity of 1 and 9%.

intervals (times of waiting for the next pulse t) were measured with the resolution of 10 ns. Fig. 2 demonstrates

the distributions of waiting times in case impact loads are applied on SiC ceramics with porosities of 1 and 9%. The distributions are constructed as $N_{AE}(t > \tau)$ dependences on τ , where N (vertical coordinate) is the number of pulses with waiting time t exceeding parameter τ that takes values of detected interpulse intervals (horizontal coordinate).

One can see that distributions plotted in double logarithmic coordinates contain log-linear segments $\log_{10} N_{AE}(t > \tau) \propto -\gamma \log_{10} \tau$ obeying the power law

$$N_{AE}(t > \tau) \propto \tau^{-\gamma}. \quad (1)$$

Here γ is the slope of linear segments depending on the contributions of relatively „short“ and „long“ intervals between AE pulses: the more is the slope, the less is the number of long intervals. Fig. 2 shows that the sample with the higher porosity is characterized by shorter intervals between sequential pulses.

Function $N_{AE}(t)$ in equation (1) is the unique solution of scaling equation

$$N(\lambda t) = \lambda^{-\gamma} N(t), \quad (2)$$

where λ is the scaling factor. The self-similar temporal pattern of microdamage accumulation arises due

Peak positions of acoustic and electromagnetic emission activities

Sample	Pores concentration, %	Peak position AE, μs	Peak position EME, μs
SiC1	1	40	500
SiC9	9	290	800–900

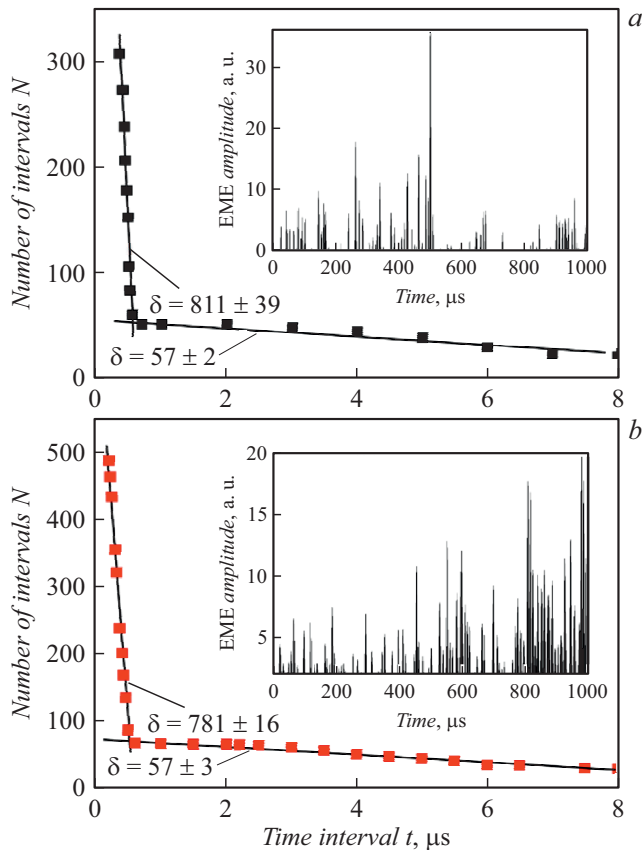


Figure 3. Temporal series of EME pulses initiated by impact loading of SiC ceramics with porosities of 1 (a) and 9% (b) (see the insets), and corresponding time distributions of interpulse intervals.

to „long–range“ interactions between multiple individual failures when the time of elastic excitation decay during the microcrack formation is longer than the time of waiting for the next crack formation.

Time scans of activity of EME occurring during microcrack relaxation are shown in Fig. 3 (in the insets). Comparison of positions of the dominant peaks in AE (Fig. 1) and EME scans shows a considerable time lag of the EME temporal series onsets with respect to those of AE (see the Table). The lag value is related to the lifetime of open cracks.

Dependences of the number of intervals (and, respectively, the number of EME pulses) $N_{\text{EME}}(t > \tau)$ on τ were linear

$$N_{\text{EME}}(t > \tau) \propto -\delta\tau, \quad (3)$$

each consisting of two segments with different slopes (Fig. 3). The major part of EME pulses were arising after intervals shorter than $1 \mu\text{s}$ (such pulses gave almost vertical curves), while a small number of longer pulses arising after long intervals (1 to $8 \mu\text{s}$) fitted a low–slope curve. Distributions consisting of pairs of $N_{\text{EME}}(t > \tau)$ dependences on $\delta\tau$ (Fig. 3, a and b) evidence for the presence of microcracks of two types with different relaxation rates. This phenomenon may be explained by that the impact damage of a porous material is accompanied by generation of both quickly relaxing ($\sim 1 \mu\text{s}$) tiny cracks in the grain bulk and larger and more stable (up to $8 \mu\text{s}$) cracks interconnecting grains.

Comparison of distributions of time intervals between the microcrack nucleations in the impact–loaded heterogeneous material (SiC ceramics) showed that their accumulation is statistically time–correlated: the microcrack formation affects the time of waiting for a new crack nucleation (AE data). Annihilation of an individual electric charge during crack collapsing after the shock wave passage is independent of annihilation of other charges.

Conflict of interests

The authors declare that they have no conflict of interests.

References

- [1] S.I. Yun, S. Nahm, S.W. Park, *Ceram. Int.*, **48** (1), 1429 (2022). DOI: 10.1016/j.ceramint.2021.09.244
- [2] J. Wade, S. Ghosh, P. Claydon, H. Wu, *J. Eur. Ceram. Soc.*, **35** (6), 1725 (2015). DOI: 10.1016/j.jeurceramsoc.2014.12.030
- [3] M.M. Davydova, S.V. Uvarov, O.B. Naimark, *Phys. Mesomech.*, **19** (1), 86 (2016). DOI: 10.1134/s1029959916010094.
- [4] J.H. Eom, Y.W. Kim, S. Raju, *J. Asian Ceram. Soc.*, **1** (3), 220 (2013). DOI: 10.1016/j.jascer.2013.07.003
- [5] J.L. Zinszner, P. Forquin, G. Rossiquet, *Int. J. Impact Eng.*, **76**, 9 (2015). DOI: 10.1016/j.ijimpeng.2014.07.007
- [6] D. Das, N. Kayal, *J. Mater. Sci. Res. Rev.*, **2** (2), 1 (2019).
- [7] D. Song, Q. You, E. Wang, X. Song, Z. Li, L. Qiu, S. Wang, *Geomech. Geoeng.*, **19** (1), 49 (2019). DOI: 10.12989/gae.2019.19.1.049
- [8] K. Eftaxias, V.E. Panin, Ye.Ye. Deryugin, *Tectonophysics*, **431** (1–4), 273 (2007). DOI: 10.1016/j.tecto.2006.05.041
- [9] H. Zhao, Z. Liu, Y. Yang, X. Liu, K. Zhang, Z. Li, *Trans. Nonferr. Met. Soc.*, **21** (6), 1329 (2011). DOI: 10.1016/S1003-6326(11)60861-3
- [10] S.I. Yun, M.R. Youm, S. Nahm, S.W. Park, *Ceram. Int.*, **37** (9), 11979 (2021). DOI: 10.1016/j.ceramint.2021.01.040